Non-Adiabatic Flamelet Modeling for Combustion Processes of Oxy-Natural Gas Flame

Gunhong Kim, Yongmo Kim*

Department of Mechanical Engineering, Hanyang University, 17 Haengdang-dong, Seongdong-gu, Seoul 133-791, Korea

In order to realistically predict the combustion characteristics of the oxy-fuel flame, the present study employs the non-adiabatic flamelet approach. In this combustion model, the detailed equilibrium chemistry is utilized to accurately account for the thermal dissociation as well as to properly include the radiative cooling effects on the detailed chemistry. Numerical results indicate that the present approach has the capability to correctly capture the essential features and precise structure of the oxy-fuel flames. In this work, the detailed discussion has been made for the characteristics of oxy-fuel flames, the capability and defect of the present approach and also uncertainties of experimental data.

Key Words : Oxy-Fuel Combustion, Flamelet Model, Probability Density Function, Radiative Heat Transfer, Unstructured-Grid Finite Volume Method

1. Introduction

Recently the industries have been driven by the requirements of maintaining or improving product quality and minimizing production costs. Within these requirements, the overall energy management and energy efficiency play important roles. It means that new, high-performance designs will provide smaller, more compact furnaces offering lower capital investments. In designing or selecting high-efficiency furnaces, several environmental aspects must be taken into account. These include considerations on emissions of carbon dioxide, carbon monoxide and nitrogen oxides. The most recent regulations of the Kyoto conference impose on industrialized nations reductions of carbon dioxide emissions.

Over past 10 years, oxy-fuel combustion has gained widespread acceptance as an alternative to the conventional air-fuel firing. Initial concerns over furnace refractory life due to higher flame temperatures and combustion space concentrations, and continuous and costly burner maintenance have largely been overcome. The level of oxy-fuel usage is expected to increase as the perceived risks and costs are reduced with more experience and improved combustion technology, furnace design, and air separation technology. Today, both oxy-fuel and air-fuel furnaces are able to meet existing regulations. However, it is acknowledged that oxy-fuel has the potential to reduce costs and achieve lower emissions simultaneously (Lievre, 2001).

Different to the air-fuel case, designers of oxy-fuel burners still rely heavily on engineering intuition and trial and error testing procedures. This is due both to the scarcity of comprehensive experimental data in semi-industrial and full-scale combustion systems and to the limited capabilities of existing CFD codes, whose predictions cannot be used with confidence to assist in the furnace/burner design process (Lallemant et al., 2000). With regard to numerical research, there have been only the limited publications to

* Corresponding Author,
E-mail : ymkim@hanyang.ac.kr
TEL : +82-2-2220-0428; **FAX** : +82-2-2297-0339
Department of Mechanical Engineering, Hanyang University, 17 Haengdang-dong, Seongdong-gu, Seoul 133-791, Korea. (Manuscript **Received** January 14, 2005; **Revised** August 10, 2005)

deal with predicting the detailed structure and properties of oxy-natural gas flames. However, the previous numerical approach (Brink et al., 2000; Breussin et al., 2000) for the oxy-fuel flames was based on the relatively ad-hoc physical models concerning the turbulent combustion processes and the detailed thermo-physical properties. At the high temperatures prevailing in oxy-fuel combustion, the chemical dissociation and radiative heat transfer as well as flame/radiation interaction are progressively dominant. Thus, in modeling the oxy-fuel flames, the chemistry model must have a capability to fully account thermal dissociation. Moreover, since the flue gases mostly consisting of H_2O, CO_2 and CO, which are known as strongly radiating species, the energy loss effects on the turbulent combustion model must be treated adequately.

In order to realistically treat the turbulence-chemistry interaction encountered in the oxy-fuel flames, the present study employs the non-adiabatic flamelet approach. In this combustion model, the detailed equilibrium chemistry is utilized to accurately account for thermal dissociation as well as to properly include the radiative cooling effects on the turbulent combustion model (Young and Moss, 1995). To address the dominant mode of energy transfer in these high temperature equipments, the radiative heat transfer is calculated by using the finite volume method (FVM), which has been known to provide accurate results in planar, 3D geometry, and axisymmetry by using both the structured grid and the unstructured grid (Raithby and Chui, 1990). All physical models, which include flamelet model and radiation, have been implemented into our flow solver of the unstrucuted-grid finite volume method.

In the present work, we have chosen the measurements of the OXYFLAM project (Lallemant et al., 1997) to check the predictability of our developed code. The OXYFLAM project was motivated to generate a detailed set of information for designing the burners and validating computer codes for oxy-fuel flame calculations. Based on numerical results, the detailed discussions have been made for the essential features of oxy-fuel combustion, the capability and defect of the present numerical approach and also uncertainties of experimental data.

2. Mathematical Formulation

2.1 Non-adiabatic flamelet approach

Since the detailed descriptions of the conserved scalar/probability density function (PDF) approach are given by many other literatures (Spalding, 1971; Bilger, 1976), only the fundamental concept and the non-adiabatic equilibrium calculation regarding to heat loss/gain will be outlined in this paper. The basic idea of the model is the numerical separation of fluid dynamics and chemistry introducing a chemistry-independent conserved scalar variable called the mixture fraction, which is zero in the oxidizer stream and one in the fuel stream generally in a two-feed system.

In the equilibrium chemistry approach, all the instantaneous thermochemical properties are calculated by computing the equilibrium state of the detailed chemistry, and are stored in an equilibrium library prior to a flame calculation. At adiabatic flame condition with no radiative heat loss, all the interested values of flame can be immediately determined only by mixture fraction. When heat loss is taken into account, however, the local value of enthalpy depends not only on mixture fraction but also on the balance of enthalpy energy transport. In that case, an additional transport equation has to be solved for enthalpy as an independent variable. For calculating a non-adiabatic nonpremixed flames by using the equilibrium chemistry, the equilibrium flame-library must be confirmed to have the values of all possible energy states. Therefore additional variable will be needed to represent the heat loss or gain states. In this study, we address the normalized enthalpy loss variable approach (Louis et al., 2001) as defined below

$$\zeta=\frac{h-h_{\min}}{h_{ed}-h_{\min}}=\frac{h-h_{\min}}{U(Z)} \tag{1}$$

where h_{ad} is the adiabatic enthalpy and $h_{\min}$ the minimum value of the enthalpy, which is

defined as the enthalpy of the mixture when instantly cooled down to the temperature of the surrounding. Subsequently, the enthalpy loss variable, ζ, represents the local fraction of radiative or convective heat losses. In the adiabatic case, this enthalpy loss variable remains unity. When heat loss is taken into account, ζ will be smaller than unity. Through this method, the non-adiabatic equilibrium database can be constructed easily from the adiabatic state to the maximum cool-downed state. Constructing the flame database using the equilibrium chemistry, the basic idea is to modify the enthalpy values according to the normalized enthalpy loss variable and to calculate the equilibrium chemistry at the prescribed enthalpy profiles.

These similar processes have been explained in more detail by Carpentier et al.(2003), who calculated the non-adiabatic flamelets by modifying not the normalized enthalpy loss variable but the radiative sink term of the flamelet equation. In Figure 1 the cooling effects on oxy-methane flame are illustrated in the cases of flame temperature and the CO and CO_2 concentrations, especially considering detailed equilibrium chemistry. Decreasing the enthalpy loss variable, temperature has the tendency to decrease because of the proportionality of temperature to enthalpy. With regard to CO and CO_2, the variations are clearly seemed sensitive to enthalpy loss or temperature. Toward low temperatures, less CO equilibrium is produced and consequently more CO_2 is produced. As the flamelet library displayed in Fig. 1, the non-adiabatic approach with detailed chemistry is needed to accurately predict the temperature and gas compositions in the context of high-temperature and strongly radiating flames. Through this work the detailed chemistry of GRI-Mech Version 2.11 is used for constructing the non-adiabatic equilibrium library.

Assuming that enthalpy and mixture fraction are statistically independent, the enthalpy equation is now transformed to a new enthalpy loss variable that is to a large extent statistically independent of the mixture fraction. Substituting the enthalpy loss variable of Eq. (1) in the enthalpy transport equation gives the following

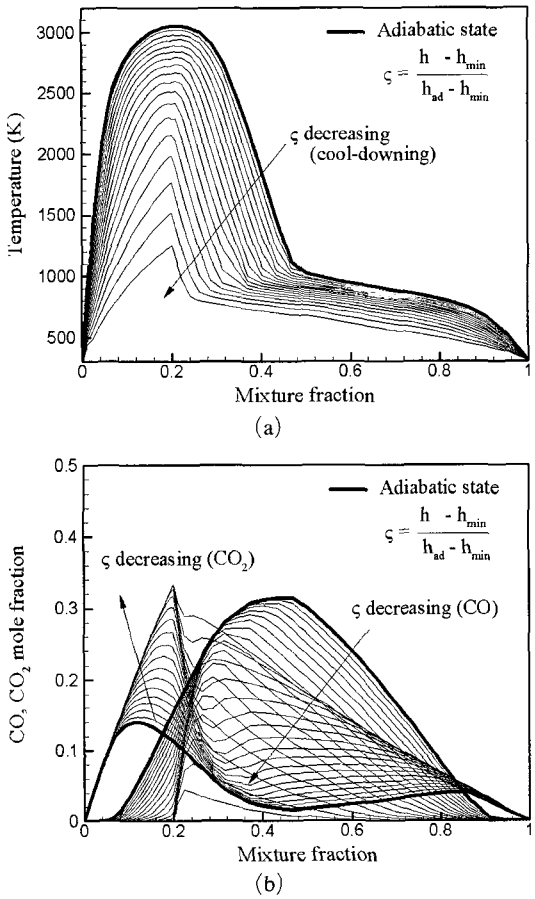

Fig. 1 Non-adiabatic equilibrium library for CH_4-O_2 chemistry

mean value equation for ζ:

$$\frac{\partial \bar{\rho}\widetilde{\zeta}}{\partial t}+\nabla\cdot(\rho\tilde{\boldsymbol{u}}\tilde{\zeta}) =-\nabla\cdot[\rho D_t\nabla\tilde{\zeta}]+\frac{1}{2}C_{g2}\frac{\tilde{\varepsilon}}{\tilde{k}}\bar{g}(\tilde{\zeta}-1)\frac{\lambda}{c_P}\frac{\widetilde{U_{ZZ}}}{U}-\bar{S}_i \quad (2)$$

where $\widetilde{U_{ZZ}}$ denotes the Favre average of second derivative of U to mixture fraction and $\bar{S}_i$ is the source term due to radiative heat transfer, normalized with the denominator U(Z) of Eq. (1). The second term of RHS of Eq. (2) is modeled as in the mixture fraction variance equation (Louis et al, 2001). This term, which is not familiar to the conventional Favre average transport equation, accounts for the effects of scalar dissipation along the mixture fraction space. In this work the variation of enthalpy loss variable and mixture fraction is assumed to be quite linear.

For considering the energy loss effects, therefore, the equilibrium library has two independent variables, i.e., mixture fraction Z, and enthalpy loss variable, ζ, which describe the mixing state and deviation from adiabatic condition, respectively. Thereby, to account for the effects of turbulent fluctuation on the thermo-chemical scalars including temperature, density, and species mass fractions, the Favre averaged properties of the reacting mixture are evaluated by convoluting the instantaneous properties with the joint PDF of Z and ζ:

$$\tilde{\phi}=\int_0^1\int_0^1 \phi^{Equil.}(Z,\ \zeta)\,\tilde{P}(Z,\ \zeta)\,dZd\zeta \qquad (3)$$

where $\phi^{Equil.}$ is the equilibrium solution corresponding to a given mixture fraction Z and ζ, which is constructed previous to calculation. In this study, the mixture fraction Z and enthalpy loss variable ζ are assumed to be statistically independent and the shape of PDF for the mixture fraction is presumed as the beta-function and the PDF of the enthalpy loss variable is taken as delta function with neglect of its fluctuations.

2.2 Finite-volume method for radiative heat transfer

The RTE for a gray absorbing, emitting, and scattering gas in a specified direction $\boldsymbol{s}$ at any position $\boldsymbol{r}$ may be written as (Modest, 1993)

$$\frac{dI(\boldsymbol{r},\ \boldsymbol{s})}{ds}=[\kappa(\boldsymbol{r})+\sigma(\boldsymbol{r})]I(\boldsymbol{r},\ \boldsymbol{s})+\kappa(r)\,I_b(\boldsymbol{r}) +\frac{\sigma(\boldsymbol{r})}{4\pi}\int_{4\pi} I(\boldsymbol{r},\ \boldsymbol{s}')\,\Phi(\boldsymbol{s}',\ \boldsymbol{s})\,d\Omega' \qquad (4)$$

where $I(\boldsymbol{r},\ \boldsymbol{s})$ is the radiative intensity, which is a function of position and direction; $I_b(\boldsymbol{r})$ is the black-body radiative intensity at the temperature of the medium; κ and σ are the absorption and scattering coefficients, respectively; and $\Phi(\boldsymbol{s}',\ \boldsymbol{s})$ is the scattering-phase function from the incoming $\boldsymbol{s}'$ direction to the outgoing direction $\boldsymbol{s}$. In the Cartesian coordinates $(x,\ y,\ z)$, the spatial derivative term in Eq. (4) can be written as

$$\frac{dI}{ds}=\mu\frac{\partial I}{\partial x}+\eta\frac{\partial I}{\partial y}+(idim-2)\,\zeta\frac{\partial I}{\partial z} \qquad (5)$$

where μ, η, and ξ are the direction cosines along the Cartesian coordinates x, y, and z directions, *idim* denotes the dimensionality of the problem and is equal to 2 for a 2D planar or axysymmetric geometry and 3 for a 3D geometry. All boundaries are assumed to be gray-diffuse. Under this assumption, the wall bounding the medium emits and reflects diffusely. The wall boundary intensity I_W for all outgoing direction $(\boldsymbol{s}\cdot\boldsymbol{n}>0)$ is given by

$$I_w=\varepsilon I_b(\boldsymbol{r}_w)+\frac{(1-\varepsilon)}{\pi}\int_{s\cdot n>0} I(\boldsymbol{r}_w,\ \boldsymbol{s})\,\boldsymbol{s}\cdot\boldsymbol{n}d\Omega \qquad (6)$$

where ε is the wall emissivity and the unit vector $\boldsymbol{n}$ is the surface normal pointing out of the domain.

The RTE (4) involves not only spatial differentiation but also the angular integration over the solid angle Ω. To solve this equation numerically, both spatial domain and angular domain must be discretized at first. For calculating the radiative source term of the energy equation (2), we use an accurate and efficient radiative finite-volume method applicable not only for 2D planar and 3D geometries (Kim et al, 2005) but also for 2D axisymmetric geometries using an unstructured finite volume method. The axisymmetric control volume method of Murthy and Mathur (1998) is employed in 2D axisymmetric problem. In this work, a sequential iterative approach is adopted for solutions of the radiative equatuions. The solver of the discretized equations is based on a Gauss-Seidel procedure. Finally, the radiative energy loss term for a gray absorbing, emitting, and scattering gas will be obtained from the RTE and may be written as

$$\nabla\cdot q_{\mathrm{Rad}}=\kappa(r)\int_{4\pi}[I(\boldsymbol{r},\ s)-I_b(r)]\,d\Omega \qquad (7)$$

Calculating an idealized case is implemented for the validation of accuracy in a geometry with a varying temperature medium that somewhat resembles the real furnace. This problem involves a cylindrical enclosure of 6 m long and 2 m in diameter, with black walls at constant temperature (T_W=500 K). The medium is absorbing, emitting and non-scattering and has a uniform

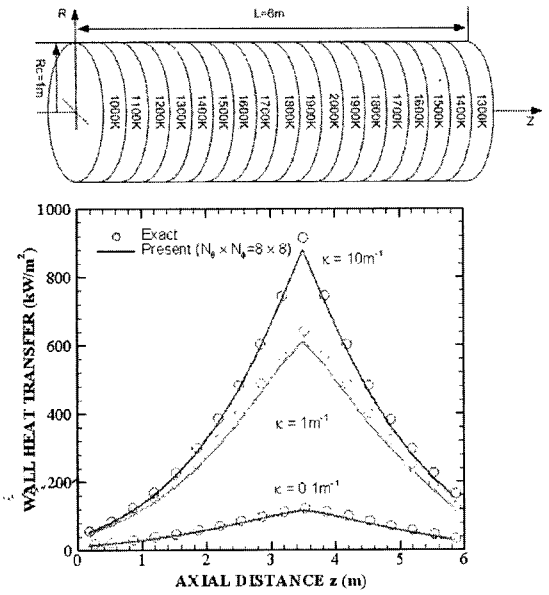

Fig. 2 The distributions of net local radiant heat transfer along the lateral wall of the cylindrical enclosure for different absorption coefficients, κ=0.1, 1 and 10 [1/m]

absorption coefficient κ. The medium temperature field is assumed known (see Fig. 2) so that the radiative finite-volume method can be decoupled from the energy equation and validated independently. The computed results of the net radiant heat transfer on the lateral wall are compared to an exact solution with using different absorption coefficients in Fig. 2. The prediction is based on a structured grid with 8 control volumes in the radial direction and 18 in the axial direction with an angular discretization of 8×8. As shown in Fig. 2, the matching order has a little difference of our prediction from that of Chui et al.(1993), but shows a good predictability.

3. Results and Discussion

As a preliminary validation case of oxy-fuel flames, a high-momentum non-swirling oxy-natural gas flame fired in the IFRF furnace 2 is chosen (Lallenmant et al., 2000). The internal length of the furnace was 3740 mm, and the dimension of the nearly square cross section was 1050×1050 mm. The chimney contraction diameter was 500 mm. The whole furnace was lined with refractory, giving a very hot flame. The natural gas entered through a round pipe in the center of the burner. The diameter of the fuel inlet was 16 mm. The oxygen stream entered through a 4 mm wide annulus. The separation distance between the oxygen stream and the natural gas stream was 6 mm. The natural gas injection velocity was 105.4 m/s and that of the oxygen stream was 109.7 m/s. The thermal input of this oxy-fuel flame was 0.78 MW.

Within the OXYFLAM project (Lallemant et al., 1997 ; 2003), the new development of measuring instruments for studying oxy-fuel flames had been undertaken extensively. Mean and fluctuating axial velocity measurements were taken using the standard IFRF water-cooled Laser Doppler Velocimetry (LDV) probe. The 25 mm diameter LDV probe and the focusing optics are enclosed in a 63 mm outer diameter water-cooled jacket which protects the equipment from the harsh flame environment. The probe end is protected from flame radiation by means of two water-cooled quartz windows located in front of the focusing lens.

A new instrument for measuring temperatures up to approximately 2500 K was also developed to overcome the limitation of existing measurement techniques for temperature measurements in excess of 2100 K in large scale combustion systems. This instrument was named the High-Temperature Suction (HTS) Pyrometer. The design and operating principle of HTS was based on the classical suction pyrometer, except that the gas is cooled before the temperature is measured by a thermocouple. In order to estimate the temperature drop in HTS pyrometer, the CARS (Coherent Anti-Stokes Raman Spectroscopy) calibration at high temperatures was conducted to enable the construction of calibration curves extending the operation of the instrument up to 2400 K. The conventional gas sampling method was used for detailed inflame determinations of major species, O_2, CO_2, UHC, CH_4, H_2, CO and NOx. Since concentrations of radicals (O, H and OH) and intermediate species (H_2 and CO)

amount to 20% of all the species in an oxy-fuel combustion, Lallemant et al.(2003) had carried out the thorough investigation into the accuracy of gas composition measurement in oxy-fuel flames and concluded that substantial measurement error is likely to occur due to radical recombination in the probe.

Numerical approaches of this oxy-natural gas furnace had been attempted by Brink et al.(2000) and Breussin et al.(2000). Just as same as done by previous calculations, the axisymmetric description is used in our try for simplification of modeling the furnace. The grid consisted of 21, 177 triangular cells, where the larger number of cells is adapted to well capture the characteristics of this jet-like flame with a large recirculating zone.

In this study, the natural gas, which consists of 86% CH_4, 5.4% C_2H_6, 1.87% C_3H_8, 0.58% C_4H10, 0.14% C_5H_{12}, 4.01% N_2, 1.79% CO_2, and 0.21% O_2 (Brink et al., 2000), is simply assumed as a pure CH_4. The modified k-ε model is used for predicting the flow and mixing fields, in which the model constants of $C_{\varepsilon 1}$ was modified from the standard value (1.44) to 1.48 to especially improve the quality of mixing field. In this preliminary calculation, a gas absorption coefficient for the equation of radiative heat transfer is obtained using the assumption of the optically thin limit throughout the whole combustion chamber. Four species H_2O, CO_2, CO, and CH_4 are taken to participate in radiation and more detailed information can be found in the web site of TNF workshop. In the previous works (Brink et al., 2000; Breussin et al., 2000), however, the constant gas-absorption coefficient 0.3 m^{-1} was used. The wall emissivities of this oxy-fuel flame with refractory liner is used just same as those of the previous numerical work (Bollettini et al., 1997). The wall emissivity of furnace is set 0.6 and the one of chimney 0.4.

Because the detailed thermal boundary conditions were given in the references (Bollettini et al., 1997), we use just the measured profile of temperature on the furnace wall, which may be similar to the temperature of recirculating flue gas. Through the present work, it is identified that this wall-temperature boundary condition is one of key factors for simulating the radiation dominant oxy-fuel flame field.

In the previous work of Breussin et al.(2000), the measured exit temperature of this oxy-fuel furnace is 1958 K and the temperature within the strong recirculating hot zone generated by the high momentum jet is around at 1850-1900 K. The predicted temperature of recirculation zone is about 1800-1920 K and the predicted temperature of the exhaust gas, 1940 K is slightly lower than the measured one. This implies that the thermal boundary conditions used in this calculation are appropriate. The predicted temperature field is displayed in Fig. 3. The most volume of chamber is filled with the hot flue gases having a nearly stoichiometric mixture are highly cooled down by the radiative and convective heat transfer. There exists little gradient of temperature at furnace wall and this tendencies are same as those observed at experiment.

In Figure 4, the quantitative comparison with measurement has been made for the profiles of axial velocity, temperature, oxygen, carbon dioxide, hydrogen and carbon monoxide. At the upstream region (x=0.22 m), the predicted profile of axial velocity has a good conformity with the measured one. However, at the downstream locations, the spreading rate of fuel jet is some underestimated. This discrepancy may be attributed mainly to the defect of the modified k-ε model.

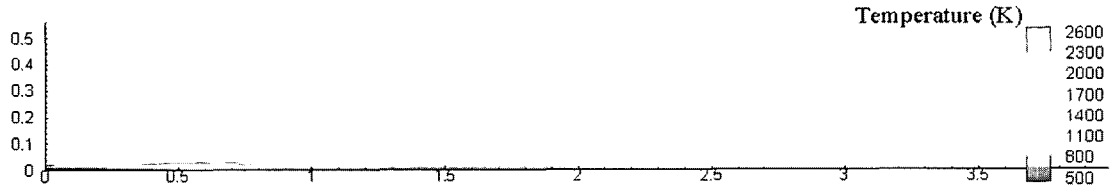

Fig. 3 Predicted temperature field of a high-momentum oxy-natural gas jet flame

In the predicted profiles of temperature, interestingly, another reaction zone is found at the upstream reaction zone (x=0.22 m). In the certain condition of the oxy-fuel flame field, this secondary reaction possibly occurs through chemical reaction between the recirculated hot-flue gases and the fresh pure O_2 stream. However, this experimental data obtained by the intrusive technique does not support the existence of this additional reaction zones. To assess the characteristics of the measured temperature distribution, Lallemant made the equilibrium calculations to estimate the gas temperature in the external recirculation zone by using the measured

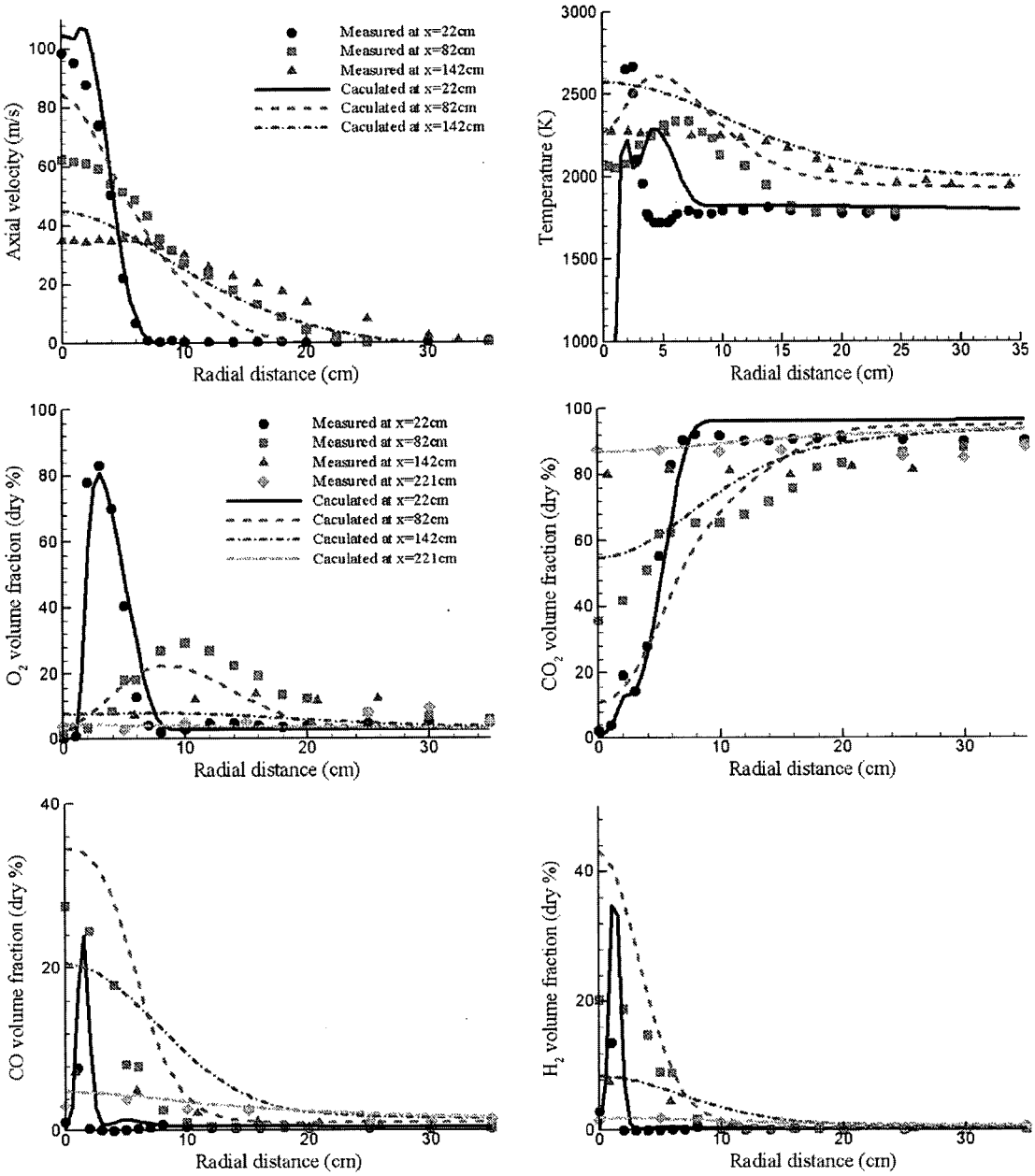

Fig. 4 Comparison between measured and predicted velocity, temperature, oxygen, carbon dioxide, carbon monoxide and hydrogen

H_2 concentrations. This estimated temperature distribution based on the measured H_2 concentrations indicates that there exists the secondary reaction zone. As illustrated in IFRF document (Lallemenat, 1997), the measured temperature after the CARS correction is quantitatively well agreed with the temperatures deduced from the H_2-equilibrium concentrations except the secondary reaction zone structure. This result might support the possible existence of the secondary reaction zone. Just like the present result at the upstream reaction zone (x=0.22 m), the curve of the calculated equilibrium temperature indicates another higher temperature region at near to fresh O_2 stream, which is not seen in the corrected temperature curve. To clarify this issue, the more systematic experimental and numerical research should be needed. At downstream locations (x= 0.82 m and 1.42 m), the temperatures are overestimated especially for the central region while those of flue gases are predicted relatively well at all radial positions. These deviated profiles of the predicted temperatures are mainly caused by the defect of the modified k-ε model. Moreover the optically thin assumption of absorption coefficient for raditive species is seemed to be another important reason, which has been known to have some errors in high-temperature ranges (TNF web site).

In terms of the O_2 mole fraction, the predicted profile well captures the measured one at all locations. It is also clearly indicated that, at downstream regions, there exist little concentrations of O_2 and the main reaction of oxy-fuel is nearly terminated. However, especially at the downstream regions (x=0.82 m and 1.42 m), the CO_2 mole fractions are considerably under-predicted due to the existence of thermally dissociated CO concentration in the high temperature condition. Evidently, the under-predictions of CO_2 concentration are closely tied with the over-prediction of temperature at these locations. Despite of the limited experimental data, the reactive intermediate species, H_2 and CO, at four locations are compared to predicted results, respectively also in Fig. 4. Same as the above statement, at the downstream (x=1.42 m) the under-predictions of CO_2 can be explained by the over-predicted results of CO in Fig. 4. The predicted and measured results of H_2 are close to each other at all locations. From Figure 4, though there exists the discrepancy of temperature, at x=0.22 the results of O_2, CO_2, H_2, and CO are well predicted to match measurements. However at downstream (especially at x=1.42 m) it seems that the over-predicted temperature causes to enforce the thermal dissociation of CO_2 to CO but the other species, O_2 and H_2, are less sensitive to this high temperature. This may mean that at this well-mixed state, nearly close to the stoichiometric mixture, the dissociation processes of CO are more important rather than H_2.

4. Conclusions

The non-adiabatic flamelet approach has been applied to predict the combustion characteristics of the oxy-fuel flame. Based on numerical results, the following conclusions can be drawn.

(1) Numerical results indicate that the present approach has the capability to correctly capture the essential features and precise structure of the oxy flames. With the more realistic gas property for radiation, the well-defined thermal boundary conditions and the improved turbulence model, the predicative capability of the non-adiabatic presumed PDF approach could be further improved.

(2) In the predicted profiles of temperature, another reaction zone is found at the upstream reaction zone (x=0.22 m). To clarify this issue, the more systematic experimental and numerical research should be needed.

(3) These deviated profiles of the over-predicted temperature are mainly caused by the defect of the optically thin assumption for radiative species, which may be very inaccurate at very high temperature.

(4) In terms of the O_2 mole fraction, the predicted profiles well capture the measured one at all locations. However, especially at the downstream region (x=1.42 m), the CO_2 mole fraction is considerably under-predicted due to the

increase of thermally dissociated CO concentration in the overestimated flame temperature.

References

Bilger, R. W., 1976, "Turbulent Jet Diffusion Flames," *Prog. Energy Combust. Sci.*, Vol. 1, pp. 87~109.

Bollettini, U., Breussin, F., Lallemant, N. and Weber, R., 1997, "Mathematical Modelling of Oxy-Natural Gas Flames," *IFRF Doc.* No. F85/y/6.

Breussin, F., Lallemant, N. and Weber, R., 2000, "Computing of Oxy-Natural Gas Flames using Both A Global Combustion Scheme and A Chemical Equilibrium Procedure," *Combustion Science and Technology*, Vol. 160, pp. 369~391.

Brink, A., Hupa, M., Breussin, F., Lallemant, N. and Weber, R., 2000, "Modeling of Oxy-Natural Gas Combustion Chemistry," *Journal of Propulsion and Power*, Vol. 16, No. 4, pp. 609~614.

Carpentier, S., Meunier, P. and Aguile, F., 2003, "A New Combustion Model with Detailed Chemistry and Heat Transfer Coupling for The Prediction of Pollutants in Gas Fired Industrial Furnaces," *Clean Air* 2003.

Chui, E. H. and Hughes, P. M. J., 1993, "Implementation of The Finite Volume Method for Calculating Radiative Transfer in A Pulverized Fuel Flame," *Combustion Science and Technology*, Vol. 92, pp. 225~242.

Kim, G. H., Kim, S. K. and Kim, Y. M., 2005, "Parallelized Unstructured-Grid Finite Volume Method for Modeling Radiative Heat Transfer," *Journal of Mechanical Science and Technology*, Vol. 19, No. 4, pp. 1006~1017.

Lallemant, N., Dugue, J. and Weber, R., 1997, "Analysis of The Experimental Data Collected during The OXYFLAM-1 and OXYFLAM-2 Experiments," *IFRF Doc.* No. F85/y/4.

Lallemant, N., Breussin, F., Weber, R., Ekman, T., Dugue, J., Samaniego, J. M., Charon, O., Van Den Hoogen A. J., Van Der Bemt, J., Fufisaki, W., Imanari, T., Nakamura, T. and Iino, K., 2000, "Flame Structure, Heat Transfer and Pollutant Emissions Characteristics of Oxy-Natural Gas Flames in The 0.7-1 MW Thermal Input Range," *Journal of the Institute of Energy*, 73, pp. 169~182.

Lallemant, N., Dugue, J. and Weber, R., 2003, "Measurement Techniques for Studying Oxy-Natural Gas Flames," *Journal of the Institute of Energy*, Vol. 76, pp. 38~53.

Lievre, K., Hewerson, R. and Hoke, B., 2001, "Recent Developments in Oxy-Fuel Firing for Glass Melters," *Glass Industry*, Vol. 82, No. 3, pp. 25~31.

Louis, J. J. J., Kok, J. B. W. and Klein, S. A., 2001, "Modeling and Measurements of A 16-kW Turbulent Nonadiabatic Syngas Diffusion Flame in A Cooled Cylindrical Combustion Chamber," *Combustion and Flame*, Vol. 125, pp.1012~1031.

Modest, M. F., 1993, Radiative Heat Transfer, Series in Mechanical Engineering, *McGraw-Hill*, New York.

Murthy, J. Y. and Mathur, S. R., 1998, "Radiative Heat Transfer in Axisymmetric Geometries using An Unstructured Finite-Volume Method," *Numerical Heat Transfere*, Vol. 33, Pt. B, pp. 397~416.

Raithby, G. D. and Chui, E. H., 1990, "A Finite-Volume Method for Predicting A Radiative Heat Transfer in Enclosures with Participating Media," *J. Heat Transfer*, Vol. 112, pp. 415~423.

Spalding, D. B., 1971, "Concentration Fluctuations in A Round Turbulent Free Jet," *Chemical Engineering Science*, Vol. 26, pp. 95~107.

Young, K. J. and Moss, J. B., 1995, "Modelling Sooting Turbulent Jet Flames Using An Extended Flamelet Technique," *Combustion Science and Technology*, Vol. 105, pp. 33~53.

Web Site of TNF Workshop, http://www.ca.sandia.gov/TNF.